PAPER • **OPEN ACCESS**

POD analysis of the wake dynamics of an offshore floating wind turbine model

To cite this article: C. Raibaudo *et al* 2022 *J. Phys.: Conf. Ser.* **2265** 022085

Journal of Physics: Conference Series **2265** (2022) 022085 doi:10.1088/1742-6596/2265/2/022085

POD analysis of the wake dynamics of an offshore floating wind turbine model

C. Raibaudo[1,2], T. Piquet[1], B. Schliffke[1,3], B. Conan[1] and L. Perret[1]

[1]LHEEA, Centrale Nantes, CNRS, Nantes, France
[2]PRISME, Université d'Orléans, Orléans, France
[3]ADEME, Angers, France

E-mail: `cedric.raibaudo@univ-orleans.fr`

Abstract. The wake dynamics of a floating wind turbine model experiencing realistic surge motion and immersed within a properly scaled atmospheric boundary layer is studied through wind tunnel experiments. The turbine is modelled by a porous disk representing the floating 2MW wind turbine located at the offshore test site in Le Croisic (France). Experiments were conducted in the LHEEA's atmospheric wind tunnel. A surge motion is imposed on the model, using a linear actuator, to replicate realistic behaviors under wave swell. Realistic frequencies of actuation are considered to study their effects on the wake properties. The wake is characterized using Stereoscopic Particle Image Velocimetry (SPIV) measurements in a y - z plane normal to the flow, at two different streamwise locations x = 4.6D and 8.1D. In addition to the documentation of the main wake statistics, the velocity fields are analyzed using Proper Orthogonal Decomposition (POD). The velocity field is decomposed into a set of spatial and temporal modes. The eigenvalues convergence is shown to be relatively slow, due to the high Reynolds number turbulent boundary layer within which the model is immersed. When varying the surge motion frequency, the spatial modes do not show any significant change in shape and amplitude. However, the spectral analysis performed on the temporal modes shows the emergence of peaks at the surge motion frequency and the overall increase of the low-frequency energy content in the Power Spectral Density, in particular for the highest frequencies of motion tested.

1. Introduction

Understanding and modeling wind turbine wakes is of crucial importance to improve and optimize the performance and lifespan of wind turbines operating in wind farms [1]. The optimization of wind farms is crucial as the space with wind resources is limited, like in Europe. Performance of wind farms depends on the environmental on-site constraints, such as canopies or urban obstacles, and also on interaction of individual wakes of downstream wind turbines [2]. For particular arrangement of wind turbines in farms, the increase of turbulence and decrease of the flow speed could lead to a loss of aerodynamical performance and fatigue rise on the mechanical components [3]. A proper modelling of the wakes is therefore of particular interest for optimal arrangement of wind farms [2].

In offshore conditions, these wake flows pose a strong challenge as they result from the complex interaction between the atmospheric boundary layer, the wake generated by the turbine itself and the effect of the wave-induced motion. However, even if large-eddy simulation (LES) approaches have been increasingly employed, their computational cost is still prohibitive for practical applications [1].

Some wake models already exist in the literature [4]. In the far-wake in particular, where downstream wind-turbine can be installed after another one, simple models are based on the wind speed deficit, which could also include the wake meandering and a turbine added turbulence model [5, 6, 7]. More complex wake models based on CFD have been developed [8], but still lack of representativity compared to the models obtained by a full CFD or experimental studies, which are both costly.

A cost-effective strategy is therefore desirable to produce a low-order representation of the wake, capable of reproducing its most salient dynamical features, namely the meandering motion of the velocity deficit attributed to the large-scale dynamics of the atmospheric boundary layer and the intrinsic wake dynamics. For this goal, modal decomposition has been used to determine low-dimensional model of the turbulent wind field [1, 9, 10, 11, 12, 13]. In particular, the Proper Orthogonal Decomposition (POD) is a well-known method to extract the most energetic coherent structures in the flow [14]. Such approaches are beneficial because a limited number of modes are necessary to describe the coherent behavior of the wake [13]. For example, POD has been applied for wakes of an infinitely long row of wind turbines [15]. The objective was to determine a reduced order model of wakes and most of all the effect of the low-frequency large structures of the boundary layer.

For floating wind turbines, modal decomposition was not much suggested yet. POD analysis was performed on generated wind fields using Mann and Kaimal turbulence models [16]. For example, Nybø et al. [17] performed similar analysis using these models and LES simulations. Progress is therefore necessary to have realistic fields reduced order models for floating wind turbines.

The present study aims at investigating the influence of the wave-generated surge motion on the intermediate wake dynamics of a wind turbine model immersed within a properly scaled offshore atmospheric boundary layer through the use of POD. This study is based on Stereoscopic Particle Image Velocimetry (SPIV or PIV-2D3C) data acquired in a cross section of the wake flow modeled in an atmospheric wind tunnel. The focus is on the dynamics and the spectral content of the temporal POD modes as it is shown that the imposed surge motion weakly impacts the main statistics of the flow and its spatial structure.

2. Experimental set-up

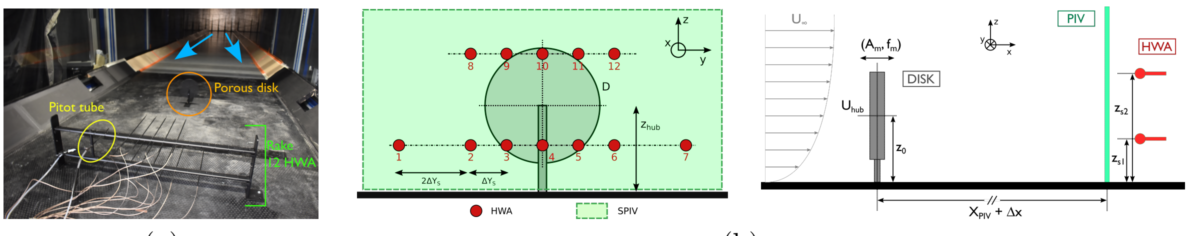

(a) (b)

Figure 1. Experimental set-up. (a) Set-up in the atmospheric wind-tunnel and (b) detailed scheme of the metrology used here.

Experiments were performed in the LHEEA's atmospheric wind tunnel. The experimental set-up is presented in Fig. 1. The free-stream incoming velocity is $U_\infty = 4.0$ m/s and the turbulent intensity about 0.5%. The boundary layer thickness is $\delta = 0.6$ m and the resulting Reynolds number based on this thickness is $Re = U_\infty \delta/\nu \approx 150000$.

The wind turbine is modeled with a porous disk of diameter $D = 0.16$ m and with the center set at a height $z_{hub} = 0.12$ m with respect to the wind tunnel floor. The model represents the floating 2MW wind turbine used in the FLOATGEN project at a scale of 1/750, with realistic geometrical parameters and flow conditions (velocity and turbulence levels in particular). FLOATGEN is installed/located at Centrale Nantes' offshore test site in Le Croisic, France. The thrust coefficient C_t is estimated to be approximately 0.5 and the power coefficient $C_p \approx 0.25$ [18]. Using porous disks for the wind-turbine wakes characterization is considered valid for the regions of investigations of this present work, at streamwise positions $x/D > 3$ [18]. A sinusoidal surge motion can be imposed on the model using a linear actuator [18]. This motion is here to replicate realistic behaviors of floating wind turbines under wave swell. The sinusoidal amplitude is $\pm$ 0.01 m and the frequencies tested $f_{act} = [0,\ 2,\ 3,\ 3.75]$ Hz. The model position is controlled retroactively and monitored, with a bias of about 1 mm between the expected and real positions [18].

The disk wake was characterized with Stereoscopic PIV in a $y - z$ plane normal to the main flow direction at two streamwise positions $x/D = 4.6$ and 8.1 downstream of the wind turbine model. The range of the final region of interest is about $3D \times 2D$ along these directions. The sampling frequency is $f_{PIV} = 14.1$ Hz and 14000 snapshots were acquired. Constant temperature anemometry (CTA) measurements using twelve single hot-wire anemometers (HWA) were also performed simultaneously to the SPIV. These measurements were used for stochastic reconstruction, but are not presented here.

3. Mean wake

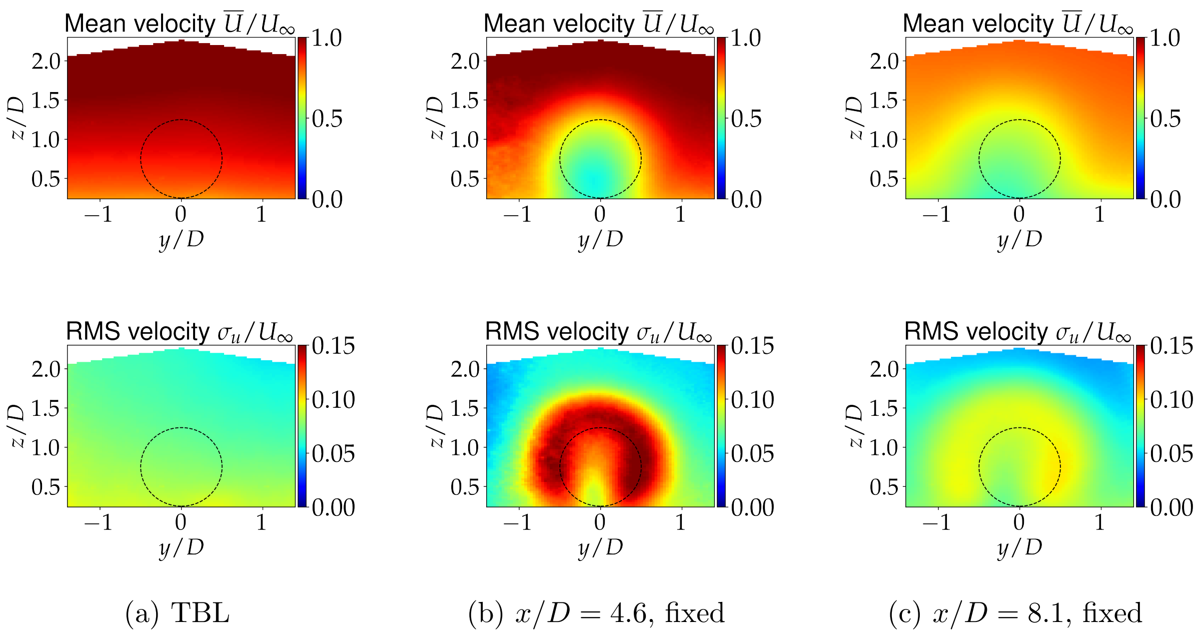

Figure 2. Streamwise mean (first line) and RMS freestream velocity σ_u/U_∞ for: (a) turbulent boundary layer without model, (b) wake for the fixed model at $x/D = 4.6$ and (c) wake for the fixed model at $x/D = 8.1$.

These PIV measurements were used to characterize the mean wake flow. Streamwise mean and RMS velocity fields σ_u/U_∞ are presented in Fig. 2. Three configurations are considered here: the turbulent boundary layer without model and the wake of the model without motion at

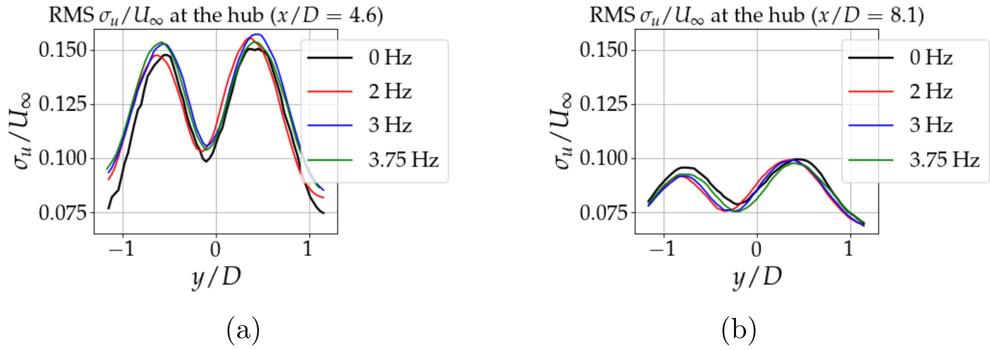

Figure 3. Streamwise RMS velocity u/U_∞ profile at hub height for the model wake for different surge motions at two PIV streamwise positions: (a) $x/D = 4.6$ and (b) $x/D = 8.1$.

two streamwise positions of the PIV set-up. Compared to the unperturbed incoming flow, the turbulence intensity increases in the near-wake from 8 % up to 15 %. The circular horseshoe shape observed in the RMS fields is classical and can be found in previous works [10]. In the streamwise direction, the wake increases in radius but decreases in turbulence intensity. A slight shift of the wake center to the negative y-direction is also observed, also seen in previous works [18, 19]. As small negative spanwise velocity $\overline{V}$ is also observed for the turbulent boundary layer, it could be due to flow structures incoming upstream the model.

Imposing a wave-induced motion for the model, as a mimic of floating wind turbines behavior, could impact on the wake dynamics. The influence of the surge motion on the mean is shown in Fig. 3. Streamwise RMS velocity σ_u/U_∞ profiles at the hub ($z/D = 0.74$) are considered for two streamwise positions and different surge motions. Compared to the fixed model ($f_{act} = 0$ Hz), in the near wake, the RMS velocity slightly increases, especially at the two main peaks. On the contrary, at the far wake, the surge motions makes the turbulence intensity slightly decreasing. The profiles are still close together, suggesting the influence of the surge motion of the mean statistics is small. Surge motions make the wake more turbulent in the near wake, and less perturbed in the far wake.

4. Proper Orthogonal Decomposition

Using POD in its snapshot version, the fluctuating velocity fields are decomposed into a set of orthogonal spatial modes $\mathbf{\Phi_i}$ and temporal modes a_i, as

$$\mathbf{u}(\mathbf{x}, t) \approx \sum_{i=1}^{N_m} \mathbf{\Phi_i}(\mathbf{x})\, a_i(t) \tag{1}$$

with N_m the number of modes used for the truncation. The methodology is applied for two streamwise positions $x/D = 4.6$ and $x/D = 8.1$, and four different frequencies of motion. The three components of the velocity $\mathbf{u} = [\ U,\ V,\ W\ ]$ are integrated in the snapshots matrix. For the streamwise position $x/D = 4.6$, the convergence of the eigenvalues are shown in Fig. 4. Compared with typical bluff-body flows, the eigenvalues convergence is relatively slow, due to the high Reynolds number incoming turbulent boundary layer. Considering different frequencies of motion, no significant difference can be observed in the eigenvalues. The observations are similar for $x/D = 8.1$, and the eigenvalues are close between the two streamwise positions.

Profiles of the spatial modes Φ_i of the streamwise velocity component along the spanwise y-direction are presented in Fig. 5. Two heights ($z/D = 0.74$ at the hub height, and $z/D = 1.25$ at the top of the porous disk) and three modes (from 0 to 2), for each streamwise position, are

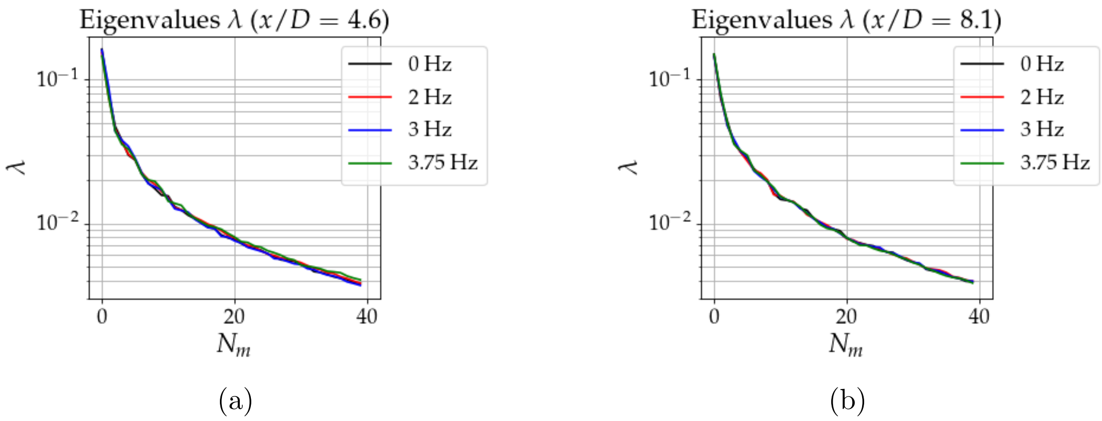

Figure 4. Eigenvalues from the POD obtained from different streamwise positions (a) $x/D = 4.6$ and (b) $x/D = 8.1$. For each configuration, four frequencies of motion are considered: 0 Hz (fixed), 2 Hz, 3 Hz and 3.75 Hz.

considered here. The influence of the surge motion on the spatial modes is also observed here with different frequencies of motion. For each plot, the sign of the spatial modes is adapted for a better understanding of the comparative study.

No significant effect of the surge-motion is therefore observed on the spatial modes of the streamwise velocity. Similar modes between the near and far wakes are also similar in shape, and close in terms of amplitude. Spatial POD modes of the transverse and vertical velocity components v and w, respectively, show the same behavior as that of streamwise component, i.e. non visible influence of the surge-motion frequency (not shown here).

However, significant differences in the temporal modes dynamics are observed in Fig. 6. Premultiplied PSD of the temporal modes a_i are shown for the first three modes and different cases of streamwise positions and motion frequencies. PSD of the temporal modes from the unperturbed flow without model are also calculated and presented in the figure. Non-dimensionalized frequency $f^* = fD/U_{hub}$ is used here, with $U_{hub} = 3.8$ m/s the velocity at the hub position without model as an usual way to dimensionalize the PSD in previous works.

For the flow without model, a broad spectrum is observed. The main peak is localized around $f \approx 1$ Hz ($f^* = 0.04$). The presence of the porous disk increases the dominant frequency of the first POD mode for both streamwise positions around $f^* = 0.13$. Traces of this spectral peak are found also in mode 2.

By introducing surge motion of the model, the wake dynamics adapts to this forced frequency. Particular behavior is observed for high-frequency surge motions. A surge motion of $f_{act} = 2$ Hz ($f^*_{act} = 0.09$) shows similar behavior as the fixed model, except localized peak around this frequency. But motions of $f_{act} = 3$ Hz ($f^*_{act} = 0.13$) and $f_{act} = 3.75$ Hz ($f^*_{act} = 0.16$) present a strong emergence of the main peak and overall increase of the spectral energy at low frequency. This is observed for the first modes and for both streamwise positions.

5. Discussions

A summary of the main peak frequencies found in the PSD is presented in Tab. 1. As explained previously, the introduction of surge motion impacts the main wake dynamics. Whatever the surge-motion frequency considered, the main PSD peak adapts to this frequency. For $f^*_{act} = 0.09$, close but different frequencies can be found in modes 0 and 1. It could be due a complex interaction between the model motion and the flow dynamics, as the natural wake and surge-motion frequencies are close. PSD of the first temporal modes show stepper slopes for higher

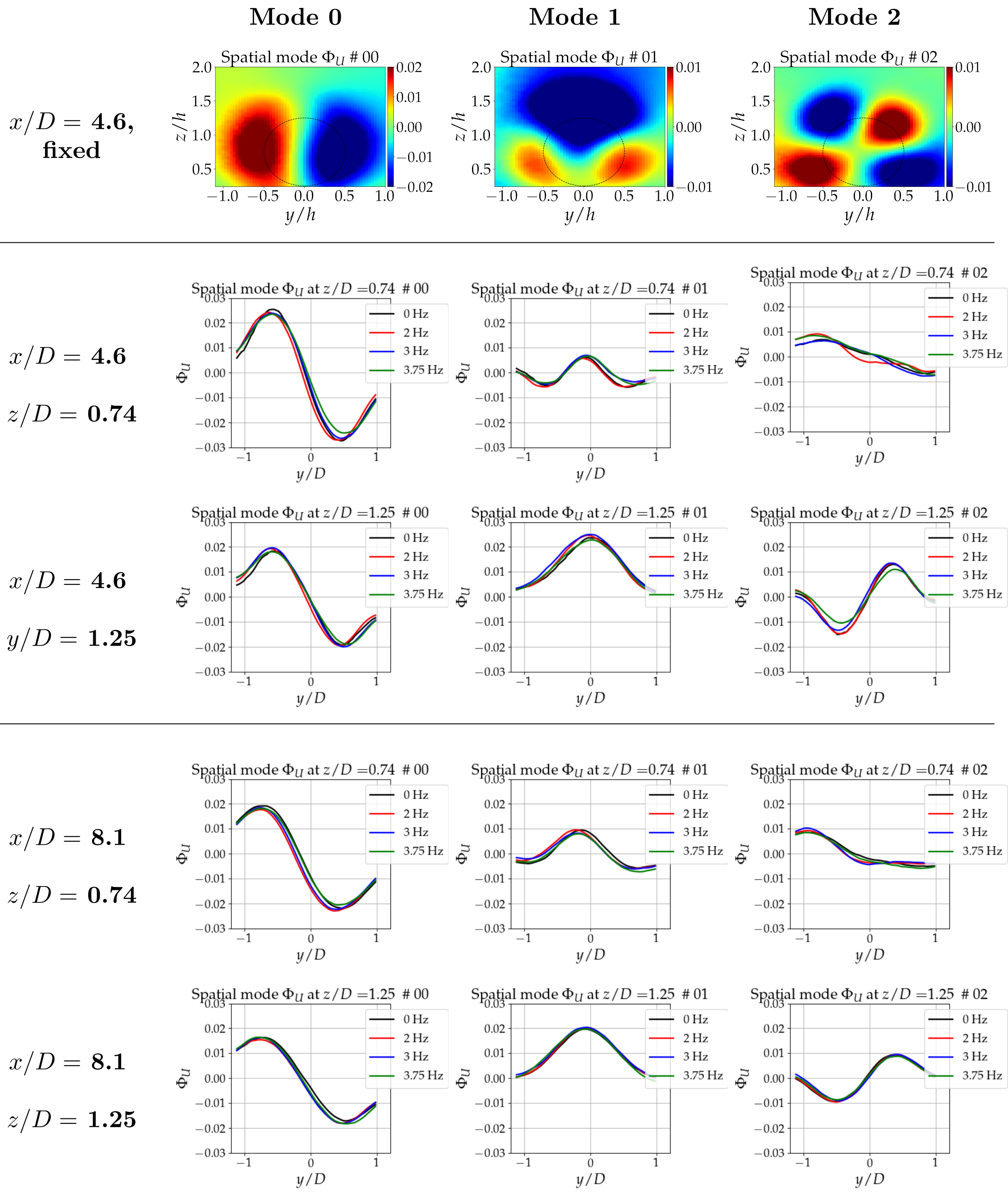

Figure 5. Profiles of spatial modes Φ_i along the spanwise y direction at two heights (the hub height $z/D = 0.74$ and the top of the model $z/D = 1.25$) for modes $i = 0$ to 2 (*columns*). For each configuration (*lines*), different frequencies of motion are considered: 0 Hz (fixed), 2 Hz, 3 Hz and 3.75 Hz.

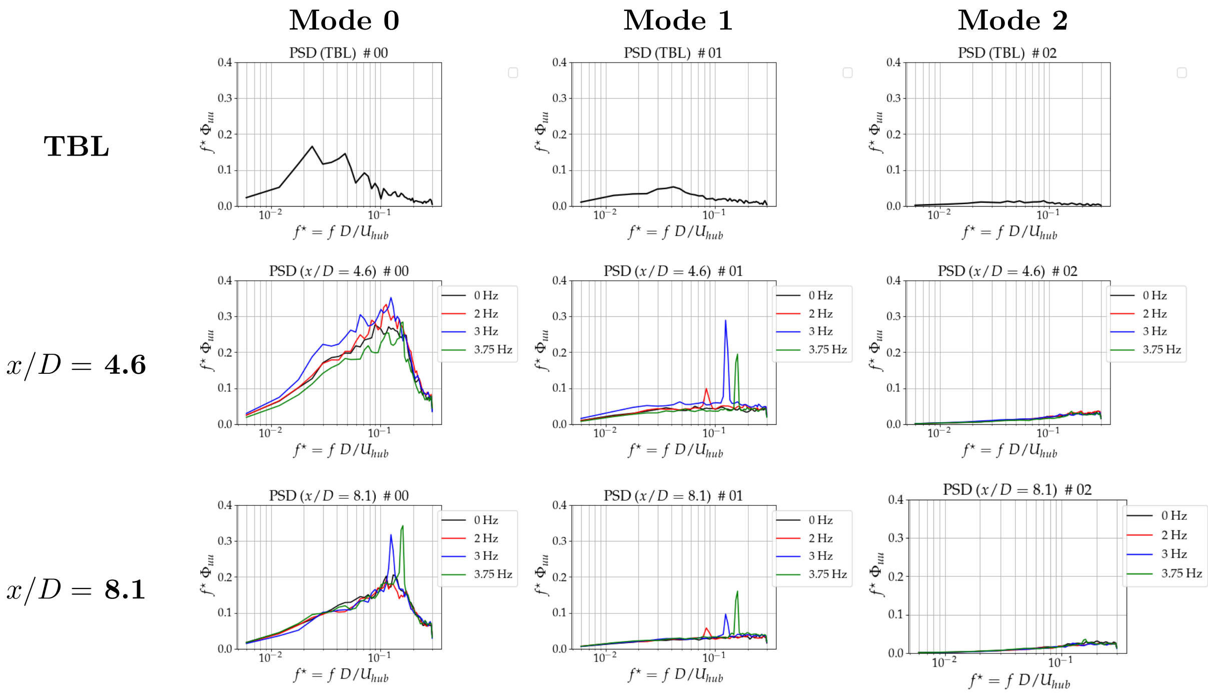

Figure 6. Premultiplied PSD of the temporal modes a_i obtained from different configurations (*lines*): (1) turbulent boundary layer without model, (2) model wake at $x/D = 4.6$ and (3) model wake at $x/D = 8.1$. The first three modes are presented for each position (*columns*): (a) mode 0, (b) mode 1 and (c) mode 2. For each configuration, different frequencies of motion are considered: 0 Hz (fixed), 2 Hz, 3 Hz and 3.75 Hz.

surge-motions frequencies ($f^*_{act} = 0.13$ and 0.16), and their dynamics more pronounced. The motion frequencies can also be found in the far wake PSD, whatever the temporal mode chosen, suggesting the consistence of the wake generated by this motion and convecting downstream. These significant peaks observed at higher frequency could correspond to a frequency-lock phenomenon between the forced frequency of the motion and the first harmonic of the natural dynamics of the wake (twice the natural main frequency).

Position x/D	**Surge motion freq.** f^*_{act}	**PSD peak frequency** f^*		
		Mode 0	Mode 1	Mode 2
TBL		0.04	0.04	0.04
4.6	0	0.09	0.07	/
	0.09	0.11	0.09	/
	0.13	0.13	0.13	/
	0.16	0.16	0.16	0.16
8.1	0	0.13	/	/
	0.09	0.11	0.08	0.17
	0.13	0.13	0.13	/
	0.16	0.16	0.16	0.16

Table 1. Summary of the main peak frequencies found in the PSD. In gray the PSD peak frequencies f^* corresponding (totally or close to) the surge motion frequency f^*_{act}.

6. Conclusions

Considering realistic conditions of the incoming flow of floating wind turbines has been proved to be of crucial importance. A proper consideration of the surge-motion in particular is important for floating wind turbines wakes. In the present study, velocity fields have been acquired experimentally by PIV for wakes of fixed and moving porous disks, corresponding to realistic conditions of offshore floating wind turbines. A modal analysis using POD was performed on the PIV fields at two streamwise positions (near and far wake) and different surge-motions frequencies.

The POD analysis showed no significant effect of the surge-motion on the spatial modes. However, the main differences in the flow dynamics between different realistic imposed surge motions mainly reside in the behaviors of the temporal modes. From a low-order modeling strategy point of view, it means that a unique set of spatial modes could be used combined with artificial temporal modes having the proper dynamics in order to generate flow fields corresponding to generic floating wind turbines.

References

[1] D. Bastine, L. Vollmer, M. Wächter, and J. Peinke. Stochastic wake modelling based on POD analysis. *Energies*, 11(3):1–29, 2018.

[2] J. Schmidt and B. Stoevesandt The impact of wake models on wind farm layout optimization. *Journal of Physics: Conference Series*, 625(1), 2015.

[3] R. J. Barthelmie, S. T. Frandsen, M. Nielsen, S. C. Pryor, P.-E. Réthoré and H. E. Jørgensen. Modelling and measurements of power losses and turbulence intensity in wind turbine wakes at Middelgrunden offshore wind farm. *Wind Energy*, 10(6):517–528, 2007.

[4] J. W. Heemst Improving the Jensen and Larsen Wake Deficit Models. *Master of Science thesis*, Delft University of Technology, 2015.

[5] N. O. Jensen A note on wind generator interaction. *Risø-M-2411 Risø National Laboratory Roskilde*, 1–16, 1983.

[6] J. F. Ainslie, R. J. Barthelmie, S. C. Pryor, S. Larsen, J. Højstrup and M. Thøgersen Calculating the flowfield in the wake of wind turbines. *Journal of Wind Engineering and Industrial Aerodynamics*, 27(1–3), 213–224, 1988.

[7] S. T. Frandsen, R. J. Barthelmie, S. C. Pryor, S. Larsen, J. Højstrup and M. Thøgersen Analytical modelling of wind speed deficit in large offshore wind farms. *Wind Energy*, 9(1–2), 39–53, 2006.

[8] J. Schmidt and B. Stoevesandt Wind farm layout optimization with wakes from fluid dynamics simulations. *European Wind Energy Association Conference and Exhibition*, 2014

[9] D. Bastine, B. Witha, M. Wächter, and J. Peinke. Towards a simplified dynamic wake model using POD analysis. *Energies*, 8(2):895–920, 2015.

[10] N. Hamilton, B. Viggiano, M. Calaf, M. Tutkun, and R. B. Cal. A generalized framework for reduced-order modeling of a wind turbine wake. *Wind Energy*, 21(6):373–390, 2018.

[11] N. Hamilton, M. Tutkun, and R. B. Cal. Low-order representations of the canonical wind turbine array boundary layer via double proper orthogonal decomposition. *Phys. Fluid*, 28:025103, 2016.

[12] S. Sarmast, R. Dadfar, R. F. Mikkelsen, P. Schlatter, S. Ivanell, J. N. Sørensen and D. S. Henningson. Mutual inductance instability of the tip vortices behind a wind turbine. *Journal of Fluid Mechanics*, 755, 705–731, 2014.

[13] K. Saranyasoontorn, and L. Manuel. Low-dimensional representations of inflow turbulence and wind turbine response using Proper Orthogonal Decomposition. *Journal of Solar Energy Engineering*, 127(4), 553–562, 2005.

[14] L. Sirovich. Turbulence and the dynamics of coherent structures. Part 1: Coherent structures. *Quarterly of Applied Mathematics*, 15(3), 561–571, 1987.

[15] S. J. Andersen, J. N. Sørensen, and R. Mikkelsen. Reduced order model of the inherent turbulence of wind turbine wakes inside an infinitely long row of turbines. *Journal of Physics: Conference Series*, 555(1), 2014.

[16] E. E. Bachynski, and L. Eliassen. The effects of coherent structures on the global response of floating offshore wind turbines. *Wind Energy*, 22(2), 219–238, 2019.

[17] A. Nybø, F. G. Nielsen, J. Reuder, M. J. Churchfield, and M. Godvik. Evaluation of different wind fields for the investigation of the dynamic response of offshore wind turbines. *Wind Energy*, 23(9), 1810–1830, 2020.

[18] B. Schliffke, S. Aubrun, and B. Conan. Wind Tunnel Study of a ”floating” Wind Turbine’s Wake in an Atmospheric Boundary Layer with Imposed Characteristic Surge Motion. *Journal of Physics: Conference Series*, 1618(6), 2020.

[19] D. Foti, X. Yang, L. Shen, and F. Sotiropoulos. Effect of wind turbine nacelle on turbine wake dynamics in large wind farms. *Journal of Fluid Mechanics*, 869, 1–26, 2019.